AAS 12-252

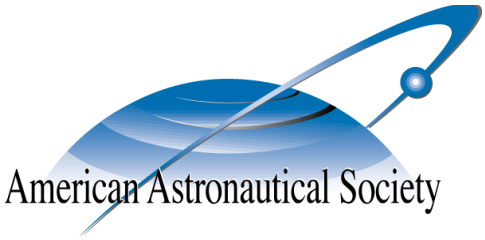

American Institute of
Aeronautics and Astronautics

TETHERED TUG FOR LARGE LOW EARTH ORBIT DEBRIS REMOVAL

Lee E. Z. Jasper, Carl R. Seubert, Hanspeter Schaub, Trushkyakov Valery and Evgeny Yutkin

AAS/AIAA Astrodynamics Specialists Conference

Charleston, South Carolina January 29 – February 2, 2012

AAS Publications Office, P.O. Box 28130, San Diego, CA 92198

(Preprint) AAS 12-252

TETHERED TUG FOR LARGE LOW EARTH ORBIT DEBRIS REMOVAL

Lee E. Z. Jasper[*], Carl R. Seubert[†], Hanspeter Schaub[‡], Trushkyakov Valery [§] and Evgeny Yutkin[¶]

The low Earth orbit debris environment continues to be a concern for the space community. While debris mitigation is an important component of reducing on-orbit clutter, active debris removal methods are likely to be necessary in the future. A debris removal system is proposed which uses fuel reserves from the second stage of a heavy launch vehicle after it has delivered its primary payload. Upon tethering to a large debris object such as another second stage rocket body, a Δv maneuver is performed to lower both objects' periapses. Specifically, a Soyuz-like rocket-body is considered the thrusting tug craft, while a Cosmos-3M rocket-body is considered the debris object. The Cosmos-3M is found to most densely populate the orbits around 700 km - 900 km between 83^o and 98^o declination. To deorbit a Cosmos-3M in 25 years from an 800 km orbit only requires a combined $\Delta v = 120$ m/s. This is within the fuel reserve budget of the Soyuz upper stage. To provide insight into the tug-debris dynamics, the tether is modeled as a spring with rigid body end masses while the tether is in tension. In order to avoid collision between the two craft, deep-space dynamics reveal that the thrust can be throttled in synchronization with the relative motion so that, at the end of a burn, zero relative velocity between the two craft is achieved. The on-orbit dynamics reveal that the orbital motion helps keep both craft separated. Further, low-thrust applications, or large initial separation distance, are shown to reduce the likelihood of post-burn collisions.

INTRODUCTION

Space debris has been an increasing hazard to orbital assets. Heavily used orbital regimes, such as sun-synchronous Low Earth Orbits (LEOs) are becoming increasingly cluttered. The LEO space environment has become significantly more cluttered with the Republic of China anti-satellite test which produced at least 2087 pieces of large debris.[1] The debris cascade effect[2] described by Kessler has begun to occur, as demonstrated by the Iridium-Cosmos collision in 2009.[3] It is therefore of paramount interest to consider methods for reducing the on-orbit debris.

Active Debris Removal (ADR) systems are likely to be required to counter the cascade effect occurring in LEO. However, Reference 4 shows that if an ADR system were active by the year 2020

[*]Graduate Research Assistant, Aerospace Engineering Sciences Department, University of Colorado, Boulder, CO 80309-0431.

[†]Graduate Research Assistant, Aerospace Engineering Sciences Department, University of Colorado, Boulder, CO 80309-0431.

[‡]Associate Professor, H. Joseph Smead Fellow, Aerospace Engineering Sciences Department, University of Colorado, Boulder, CO 80309-0431.

[§]Professor, Department of Aviation and Rocket Building, Omsk State Technical University.

[¶]post-graduated student, Department of Aviation and Rocket Building, Omsk State Technical University.

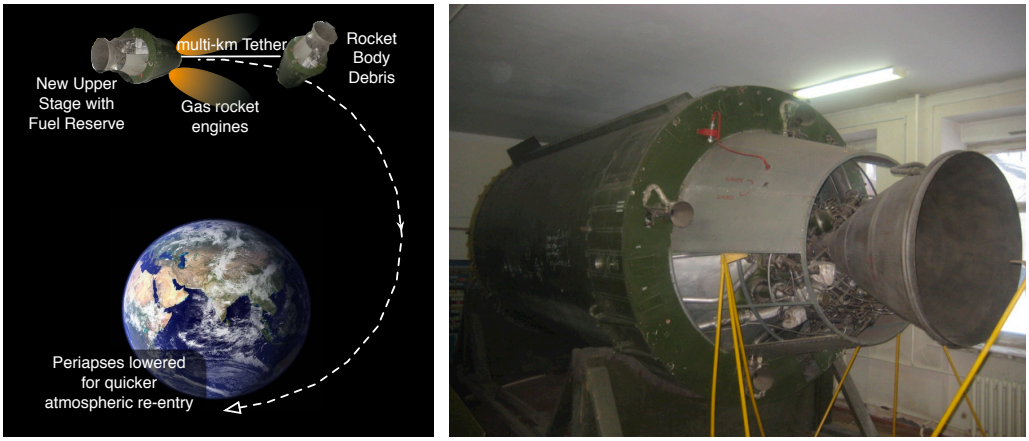

(a) Tethered Debris ADR concept (b) Second stage of SLV Cosmos-3M

Figure 1. Tethered Upper Rocket Stage Removal Concept Illustration.

the system would only need to remove five large objects a year to almost completely level off debris growth. This is encouraging, because any ADR system would only need to operate on a limited number of large debris objects. The reason that the large debris objects are of primary interest for ADR activities is that a collision of a large debris object with another spacecraft will result in a large number of smaller debris object. This debris can be small enough such that tracking it becomes a challenge, but carry enough momentum that it is poses a hazard to other operating satellites.

The task of deorbiting LEO debris translates technically into changing its orbital momentum to lower the debris' periapses. One very effective way of changing the orbital momentum of on-orbit objects is through the use of tethers. These can transfer the energy change of employing thrusters on a primary rocket to the tethered secondary object. Space tether applications have been studied for years.[5–7] Space tethers also have flight heritage with several space shuttle missions and the Small Expendable Deployer System (SEDS)[8] mission. Some of these missions have demonstrated tether deployments to lengths of tens of kilometers. It may therefore be possible to use this emerging technology application for debris removal.

The proposed tethered tug-debris system proposes to use an active upper stage rocket body to rendezvous with a debris object. This rocket is assumed to have deployed its payload and completed its primary mission. It's secondary mission goal is to use the remaining fuel reserves to rendezvous with another rocket debris object with similar orbital parameters. Next a tether is connected to the debris object, followed by an orbital momentum changing burn being applied which lowers the periapsis of both objects. The general concept, shown in Figure 1(a), will change the periapsis so that drag forces cause both objects to deorbit within 25 years. Depending upon initial starting altitude and amount of reserve fuel available to the active upper stage, the debris-tug system could be deorbited within a single orbit revolution. The tethered tug-debris architecture therefore provides a cost-effective ADR system because it deorbits two pieces of potential debris for each mission.

This paper considers the Soyuz upper stage as the "tug" craft. The Cosmos-3M rocket bodies are the large debris objects. This study investigates how much residual fuel is required to reduce the Cosmos-M type debris to decay lifetimes of less than 25 years. Further, the dynamics of the tethered system are studied in both deep-space and on-orbit to gain insight into the general behavior of the system and the effects of differential gravity. The trade-space of thrust magnitude to tether initial

(nominal) length is considered with respect to the resulting minimum separation distance between the craft. Attitudes and rotational motion of the tethered system are not considered in this study and the tether is assumed to be massless. Finite mass tethers will be considered in future work. The rendezvous and tethering of the debris object is an important task, but beyond the scope of this paper. Here the student assumes a tether has been connected to the debris object. Numerical simulations are employed to research effective configurations to apply the required net velocity change to the debris.

DESCRIPTION OF PROPOSED SOYUZ TETHERED DEBRIS REMOVAL SYSTEM

Selection of Critical Orbits for High Densities of Cosmos-3M Upper Stages

The Cosmos-3M is a universal Space Launch Vehicle (SLV). The second stage of the Cosmos-3M is shown in Figure 1(b). This heavy launch vehicle has been used to deliver space cargo to the orbits shown in Table 1. To date, there have been more than 420 launches of Cosmos-3M. Of these, 397 launches were successful, while 5 were partially successful. Of the non-successful launches, 4 emergency launches delivered the cargo space vehicle to orbit, while 18 launches failed to reach orbit.

Table 1. Cosmos-3M Orbital Parameters

Orbit	Altitude [km]	Declination [^{o}]
Circular	200 - 1700	48.5, 51, 66, 74, 83, 87.3
Elliptical	Perigee: 200 - 500, apogee: 500 - 1500	48.5, 51, 66, 74, 83, 87.3
Sun-synchronous	700-850	98.15 - 98.8

As a result, this very successful SLV has delivered hundreds of payloads into orbits with periapses as low 200-300 km, and as high as 850-1700km. At the end of its mission, after delivering its space payload, this Cosmos-3M component remains at these orbit altitudes. Space objects with periapsides above 500km will take a long time, typically more than 25 years, for their orbits to decay due to the atmospheric drag or solar radiation pressure influence. This has resulted in a significant number of large rocket bodies in these target orbits. This provides a strong motivation to investigate methods to reduce the periapsides of such space debris objects such that they will reenter the atmosphere and burn up much faster. Any proposed system will need to be able to reach these high LEO orbits, and interface with the rocket body.

An illustration of the Cosmos-3M debris at various declinations and altitudes below 2000 km is shown in Figure 2. The critical orbits where the upper stages of the Cosmos-3M rocket are most densely distributed (according to data from Table 1 and Figure 2) are identified as:

- by altitudes: 700-900 km
- by declinations: 83^o - 98^o

The long-term goal of the presented ADR method is to reduce the periapses of such Cosmos-3M bodies to 500km or below such that they will re-enter the Earth's atmosphere more rapidly. Removing such large rocket bodies will have a significant impact on the long term LEO debris population. These large objects have been identified in earlier studies as a primary source of future small debris when they collide with other space objects.

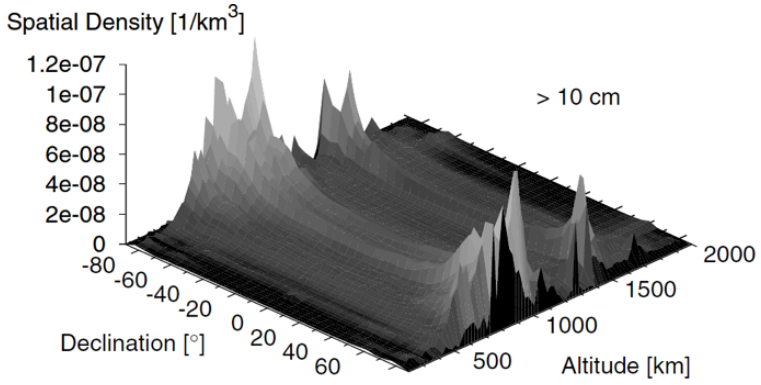

Figure 2. Spatial density in LEO versus altitude and declination for objects of diameters $d > 10$ cm according to the MASTER-2001 model, for May 2001[9]

Use of Second Stage Rockets to De-Orbit Spent Rocket Bodies from Critical Orbits

Tethered Deorbiting Method Description The proposed ADR method employs the second stages of the Soyuz launch system to lower the Cosmos-3M 2nd stages shown in Figure 1(b). The Cosmos-3M 2nd stage is referred to as the targeted separated part or SP-T, while the Soyuz upper stage is referred to as the active separated part or SP-A. The key consideration is that after the newly launched Soyuz vehicle delivers its payload to the desired orbit, it will still have a small fuel reserve. Instead of simply expelling this fuel, or deorbiting itself, the proposed concept has the SP-A actively maneuver to the SP-T object. Next, as illustrated in Figure 3, a tethered mobile component of the SP-A called the Space Micro Tug (SMT) is used to dock with the SP-T. After physically connecting to the rocket debris object, a multi-kilometer tether is tensioned prior to engaging in an orbit energy reducing burn.

The major benefit of this system is that the Soyuz system can perform two desired functions. Firstly, its primary function is to launch a new satellite into orbit. However, after performing this duty, the second stage will still have some reserve fuel amount onboard. Some of these fuel reserves are then used to maneuver the spacecraft in the vicinity of an older Cosmos-3M rocket debris object, while the remaining fuel reserve is used to lower the periapses of the tethered two-body system to a lower altitude which can yield a direct re-entry, or at least a lower orbit with a reduced re-entry time period of less than 25 years. This procedure will allow one large rocket body to be removed from the LEO population for every new spacecraft launched with the Soyuz system. Studies performed by Johnson and Liou show that the active removal of even 3-5 large debris objects per year will have a significant impact on arresting the space debris population growth.[3,4,10,11]

Studying the most critical orbits from Figure 2, a subsection of orbits are considered for further study. Let's initially consider circular orbits with altitudes from 850 to 900 km. To de-orbit the Cosmos-3M second stage space debris object (also referred to as the 'separated part' target or SP-T) within a 25 year orbit lifetime, the periapses must be lower to at least 515km. Such an impulsive orbit correction requires approximately $\Delta v = 100$ m/s. Note that the 25 year lifetime is estimated using the Cosmos-3M area-to-mass ratio of 0.0018.

After the payload separates from the SP-A (the tug craft), the SP-A performs a long distance guidance maneuver to rendezvous with the SP-T (the target debris). The SP-A then adjusts its orbit

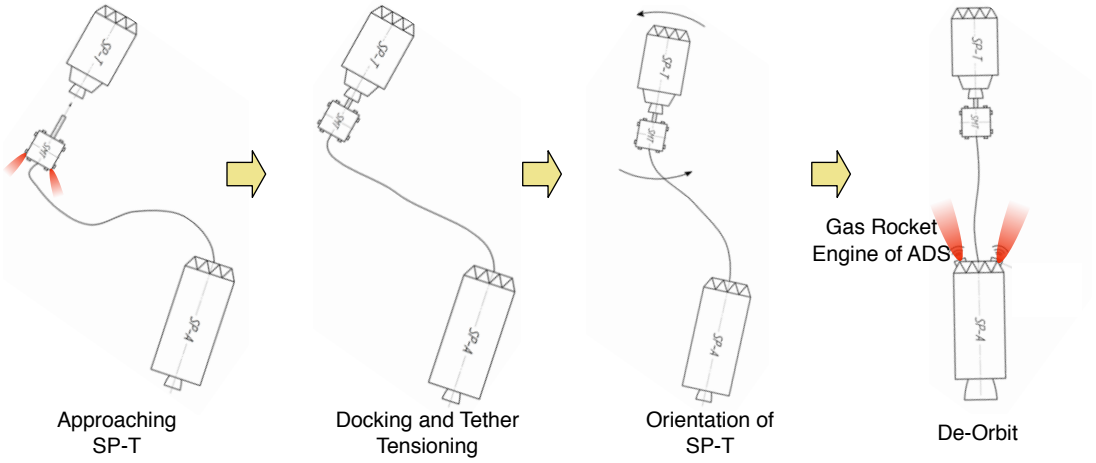

Figure 3. Illustration of a Soyuz upper stage component (ST-A) approaching and docking onto a Cosmos-3M of upper stage (ST-T) debris object, deploying a tether and engaging a periapsis lowering maneuver.

to match the orbit of the SP-T by using the active de-orbit onboard system (ADS). This maneuver is shown in Figure 4. Long-Range fuel (Δv) expenditures to approach the space debris object are above 100 m/s. The total fuel reserve of the Soyuz upper stage is not more than 200 m/s. This amount of power reserve is approximately equal to the 407.3 kg of propellant for the SP-A (see 'Soyuz' Figure 5(b)). Many studies of long distance guidance and orbital rendezvous have been conducted[12–14] and the rendezvous maneuver itself is beyond the scope of this paper. However, the time long distance approach is on the order of 1-2 orbits, approximately 3 hours. Thus, the Soyuz fuel reserve is enough to perform a rendezvous with the rocket debris, and lower its periapses from 900 to about 500 kilometers. If the space debris has a lower initial orbit radius, or more reserve fuel is carried along, then it might be feasible to have the tethered two-body system directly enter the atmosphere in a controlled way after the burn.

The docking maneuver is executed by the space micro tug (SMT). The SMT connects the SP-T and SP-A through a tether. On the SMT, there is a device installed which is used for docking with the SP-T. There are many various docking and capturing systems[15,16] that can be utilized including system 'pin-cone', androgynous peripheral attach system, harpoons, netting devices, or robotics arms. However, an in-depth study of these docking and capturing systems is left for future work. In this study it is assumed that a docking device has been developed, and the resulting relative motion of the SP-A and SP-T units are of interest. After the periapses lowering maneuver burn is completed, this study explores the resulting separation distance assuming ranges of tether lengths and materials. The flexible tether will cause interesting relative motion dynamics which couples with the orbital motion. If the two-body system has the orbit energy lower sufficiently to yield a direct re-entry into the Earth's atmosphere, then even a short term, low-speed collision of the two components will have negligible consequences. In this case, the rocket components are already on a re-entry trajectory, and the slow relative velocity is not enough to cause collision debris to remain in orbit. However, if the de-orbit burn maneuver is not sufficiently large, as considered in the example above where periapses is lowered to about 500 kilometers, then the long-term relative motion of the tethered two-body system must be considered.

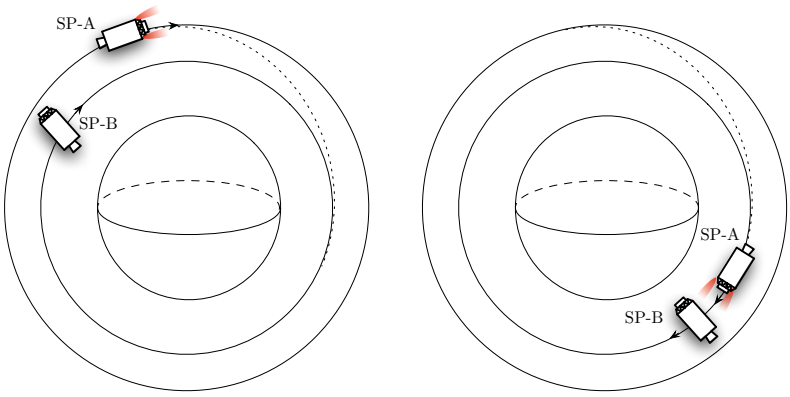

Figure 4. Illustration of a two-impulse long-range approach maneuver which sets up the active SP-A to deorbit the SP-T debris object.

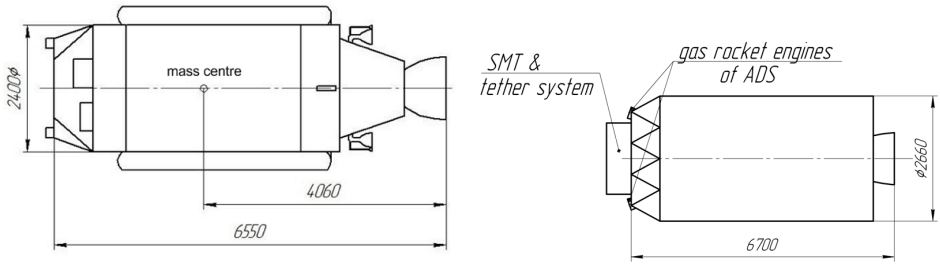

(a) Characteristics of SP-T (SLV Cosmos-3M) (b) Scheme of SP-A with ADS engines (SP 'Soyuz')

Figure 5. SP-T and SP-A Illustration and Dimensions (in units of milli-meters).

Physical Characteristics of SP-T, SP-A and ADS The overall dimensions of the SP-T and SP-A second stages are illustrated in Figure 5. The mass of the SP-T unit is about 1500kg. Table 2 provides additional approximate information on the Soyuz second stage.

Figure 6 describes the general architecture of the Soyuz ADS, which uses energy resources of unused residues of Rocket Propellant Components (RPC). The mass and inertia properties for both second stages are listed in Table 3 where the SP-A values are assumed from a cylindrical body.

DEORBIT MANEUVER REQUIREMENTS

To reiterate, if a Soyuz-like rocket stage were used to deorbit a Cosmos-like debris object, the starting altitude would likely be around 800 km and the periapses radius would occur around 500 km, assuming a $\Delta v = 100$ m/s. If there is more Δv capability or lower starting altitudes are considered, the SP-T and SP-A could both be completely deorbited. Note that the dynamics and basic behavior of the system does not vary considerably with changes in altitude. Therefore a 800 km by 500 km orbit, for the purposes of this study, does not differ much from a 500 km by 100 km orbit. The following studies consider complete 'de-orbiting' of both craft to an periapses altitude of 100 km for a direct atmospheric re-entry.

There are many requirements on the deorbiting process of satellites. ADR systems must account

Table 2. Characteristics of SP-A

Mass of construction	2355 kg
Oxidizer	Liquid oxygen
Mass of unused oxidizer	245.4 kg
Fuel	Kerosene
Mass of unused fuel	116.6 kg
Specific impulse of ADS	2000 m/s
Thrust of ADS	181.3 kg

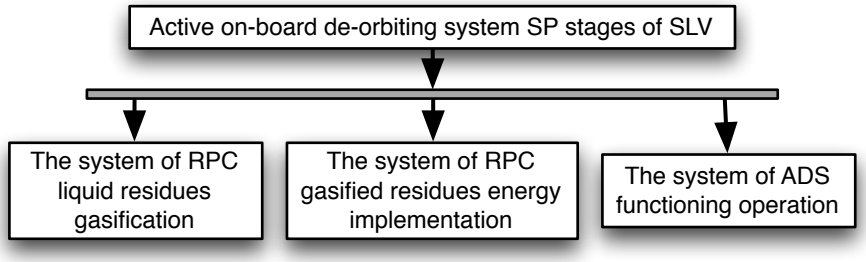

Figure 6. General architecture of ADS of SP of SLV stages equipped with main liquid propellant engine and turbo pump system for feeding propellant

for these requirements as well as system specific requirements and rules. This section details several high level requirements on any ADR system, like Δv, but also addresses several tether removal system specific requirements. While there are many considerations when deorbiting a satellite, only several concept/design requirements are considered here.

In LEO most ADR methods plan to deorbit debris into the Earth's atmosphere. Therefore most ADR methods change the energy of the objects which can be quantified using Δv. The tethered debris removal concept utilizes impulsive thrust events to deorbit debris. Therefore, a Hohmann transfer is used to compute the Δv required to deorbit the two bodies. Figure 7 shows the velocity change required to move a satellite from a given starting altitude to a 100 km altitude, at periapse. The 100 km periapse altitude was chosen as an approximate reentry altitude. The debris/tether system is assumed to start between 300 km and 1000 km circular orbits, producing required Δv's of about 50 m/s to 250 m/s. These Δv values are promising because they are relatively low and may

Table 3. Summary of Mass and Inertia of SP-A and SP-T

Object	Mass [kg]	Inertia [kg m^2]
SP-T	1500	I_{xx} = 1285 I_{yy} = 6829 I_{zz} = 6812
SP-A	2717	I_{xx} = 11365 I_{yy} = 11365 I_{zz} = 2403.1

be achieveable, even by rocket stages that have used the majority of their fuel. Figure 7 also shows that debris deorbit times, using a Hohmann transfer, are short and about 45 minutes, half the period of LEO orbits.

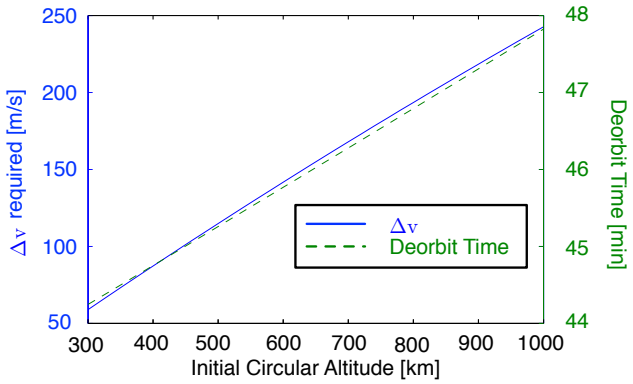

Figure 7. Δv and P_{deorbit} to reach 100 km from a given initial altitude

The thrust duration required Δt depends upon the Δv required, as well as the thrust T and system mass M. Starting from the basic force equation $F = Ma = T$ and assuming a constant thrust and system mass Eq. (1) is used to calculate the thrust duration. While the total system mass will change due to thrusting, it will be relatively small given the required Δv from Figure 7.

$$\Delta v_{\text{desired}} = \frac{T}{M}\Delta t \tag{1}$$

Therefore, if $M = 4217$ kg and the desired $\Delta v = 120$ m/s, for a 5 kN thrust, the burn time required is 101.3 seconds. Burn time is directly proportional to thrust and as thrust increases, burn time decreases. Note, that if the deorbit period is approximately 45 minutes (Figure 7), 72 seconds is only 3.7% of the total deorbit period.

Using the basic 'rocket equation' in Eq (2) an estimate of the mass used, and burn time, can be made. In Eq. (2) I_{sp} is the specific impulse of the rocket, g_0 is 9.81 m/s^2, M_0 is the initial total system mass and M_1 is the final total system mass. Rearranging Eq. (2) to solve for M_1, the total system change in mass can be found. Using the $I_{\text{sp}} = 359$ s for the third stage of the Soyuz 2.1b launch vehicle[17] , an initial system mass of 4217 kg, and a desired $\Delta v = 120$ m/s with $T = 5$ kN, the post burn mass is $M_1 = 4075$ kg. Using Eq. (1) and plugging in this new mass (assuming it is constant) produces a burn time of 97.8 seconds. This shows that the change in burn time is only a few seconds. The burn time will actually change less than this calculation predicts because the mass will originally be at M_0 and transition to M_1. Having an average system mass larger than M_1 in Eq. (1) will make the burn time closer to 100 seconds. Therefore, assuming mass does not change for these Δv's is a reasonable assumption for this gross dynamical study.

$$\Delta v = I_{\text{sp}} g_0 \ln\left(\frac{M_0}{M_1}\right) \tag{2}$$

While burn time, Δv and deorbit time are all good quantative measures of this system's required performance, there are several more qualitative requirements that need to be considered. Perhaps

the most critical aspect of post-burn relative motion is the avoidance of collision between the tug and the debris. The tether system will behave similar to a spring-mass system due to the elasiticity in the tether material. External forces, such as thrust, will expand the system, placing energy into the spring. However the lack of forces on the system in the post-burn phase will cause the spring to contract, bringing both craft together. This issue is studied in more detail in the following sections. However, one potential requirement on the tether debris removal system is that both objects shall deorbit into the atmosphere before collision occurs. A more crude, but possibly effective requirement is to ensure the required deorbit Δv is applied to both objects before a potential collision occurs. This way, even if collision occurs, both objects should have the correct energy to completely deorbit. If relative collision velocity is low, damage to both spacecraft may be minimal and all desired mass would still be removed from orbit. Further study of ejected debris from a collision needs to occur to determine whether the ejected particulates would indeed reenter the atmosphere or if they would continue to orbit.

Knowledge of the debris' mass may not be accurate. If a rocket body is being deorbited its remaining fuel mass may not be well known due to (lack of) venting. Therefore the tether system must be designed such that a fairly wide range of values can be deorbited properly. A more massive debris object will increase fuel requirements, and therefore burn time, to achieve the desired Δv. The tug craft must have sufficient fuel onboard to correct for larger masses while ensuring that deorbit occurs before collision between the two objects. If the debris mass is less than expected, this may also increase the chances of collision due to the tether force accelerating the smaller mass more quickly than expected. Also, a smaller mass would require burn time adjustment to achieve the desired deorbit location on the Earth to avoid population centers.

The debris' inertia and the attachment location are an additional consideration. Like the mass, the knowledge of the inertia of the system may vary. Inertia is important because the tether system transfers energy from the thrusting tug craft, through the tether to the debris. If the attachment point is not located at the debris' center of mass, some rotation will be induced. Energy placed into rotating the debris is energy that is not used to deorbit the debris. More importantly, any rotation of the debris may cause tangling with the tether. This will change the dynamics of the system, possibly unpredictably causing unexpected collisions. Tangling of the tether may also put stress on parts of the debris that become entangled. Components like solar panels or antennas may be broken off because the tether has wrapped around it, creating more unintentional debris in orbit. Further, the attachment location may be close to the unstable inertia axis. Thus the torque created by the tether may induce an unstable spin on the debris, again increasing the chance of tangling with the debris. Therefore the tether system must be robust to uncontrolled rotation of the debris while avoiding tangling. Studies of the tangling of the debris is beyond the scope of this paper.

SIMPLIFIED DYNAMIC TETHERED-SYSTEM ANALYSIS

The system described in this paper may be considered a 0^{th} order model of the system. A linear 'spring-mass', or 'tether-mass', system is considered (Figure 8) as substitution for the full tether dynamics. The reduction in complexity has been made due to the philosophy that simplicity can yield insight into the behavior of a system. The use of the spring-mass model has allowed for the identification of the amount of flexing expected in the tether, when and how potential collision events occur, the affets of thrusting, and the affects of initial separation distance.

While the system behavies like a spring-mass when in tension, without tension, a tether provides no force. This creates a piece-wise function with behavior that is not as easily modeled as the

nominal spring-mass system. Therefore the model is placed into a deep space environment so the pure dynamcis of the piece-wise spring-mass system can be analyzed and closed form solutions can be found. Then, the system is placed into orbit and the effects of orbital accelerations and differential gravity are observed.

Equations of Motion of the Tethered Rigid Body System

The tether system is modeled as a spring-mass (point mass) system and is modeled that way due to the tether's elasticity. The tether itself is considered massless, linear spring. Initial analysis include no orbital motion and assumed a deep space environment. Figure 8 shows a basic diagram of the satellite-tether system.

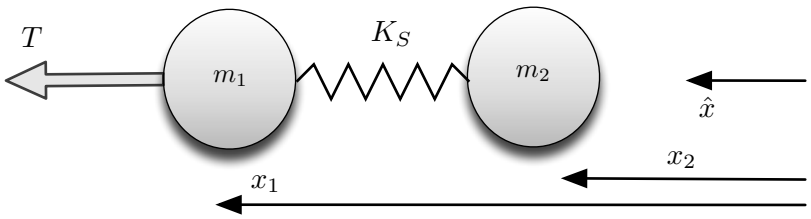

Figure 8. Spring-mass system with constant thrust

Using the spring-mass assumption, the equations of motion, given in Eq. (3) are derived by summating the forces. These equations, as written, assume one dimensional motion. However, Eq. (3) can be easily expanded to three dimensional, translational motion by simply expressing the position with a position vector $\boldsymbol{x} = [x_i, x_j, x_k]$, the mass as a diagonal mass matrix, and the spring constant as a diagonal matrix if $\boldsymbol{x}$ is defined as pointing along the spring axis.

$$\begin{bmatrix} m_1 & 0 \\ 0 & m_2 \end{bmatrix} \begin{bmatrix} \ddot{x}_1 \\ \ddot{x}_2 \end{bmatrix} + K_S \begin{bmatrix} 1 & -1 \\ -1 & 1 \end{bmatrix} \begin{bmatrix} x_1 \\ x_2 \end{bmatrix} + K_S \begin{bmatrix} -1 \\ 1 \end{bmatrix} x_0 = \begin{bmatrix} 1 \\ 0 \end{bmatrix} T \tag{3}$$

Eq. 3 only holds while $x_1 - x_2 > x_0$, where x_0 is the craft initial separation where the tether is taut but unstretched with a length L_0, because tethers do not create any forces when in compression. When the tether is slack, the equations of motion become:

$$\begin{bmatrix} m_1 & 0 \\ 0 & m_2 \end{bmatrix} \begin{bmatrix} \ddot{x}_1 \\ \ddot{x}_2 \end{bmatrix} = \begin{bmatrix} 1 \\ 0 \end{bmatrix} T \tag{4}$$

Of course, after the burn time (Δt in Eq. (1)) has passed, the thrust T becomes zero for both Eq. (3) and Eq. (4). To gain some insight into the behavior of the system, the equations are expressed as changes in separation distance x. If the separation distance relationships are:

$$x = x_1 - x_2 \tag{5}$$

Taking two time derivatives of Eq (5) yields:

$$\ddot{x} = \ddot{x}_1 - \ddot{x}_2 \tag{6}$$

where $\ddot{x}_i$ is from Eq. (3). Substituting $\ddot{x}_i$ into Eq. (6) gives the expression for the separation distance:

$$\ddot{x} = -Cx + CL_0 + \frac{T}{m_1} \tag{7}$$

where:

$$C = \frac{K_S(m_1 + m_2)}{m_1 m_2} \tag{8}$$

Eq. (7) can be solved for an analytical solution. If the initial separation distance is assumed to be $x[t = 0] = x_0$ and the initial velocity to be zero, $\dot{x}[t = 0] = 0$, then the analytic solution for x is:

$$x(t) = \frac{\frac{T}{m_1} + CL_0 - \frac{T}{m_1}\cos(\sqrt{C}t) + C\cos(\sqrt{C}t)(x_0 - L_0)}{C} \tag{9}$$

Again, this solution is only valid when there is tension in the tether. Note that L_0 is assumed to be the initial starting position x_0 for this system which simplifies the equation to:

$$x(t) = \frac{\frac{T}{m_1} + CL_0 - \frac{T}{m_1}\cos(\sqrt{C}t)}{C} \tag{10}$$

Eq. (10) can provide insight into several of the basic behaviors of the system. If the cosine term reaches reaches its maximum value of 1, then the separation distance simply becomes the initial separation L_0. Therefore, the separation will never become less than L_0 while thrusting. The maximum separation distance (when the cosine term becomes zero) is simply a ratio of the thrust, initial separation distance, the spring constant and the mass.

The spring constant is calculated using Eq. (11) where the material properties of the tether are: elasticity E, cross sectional area A, and the initial starting length L_0.

$$K_S = \frac{EA}{L_0} \tag{11}$$

Two candidate space tether materials are considered. The corresponding tether material properties used throughout this report are given in Table 4. To consider whether the massless tether assumption is reasonable, the largest values from Table 4 are used to calculate the total tether mass for a given tether length. Using Kevlar's larger density, and the larger of the area ranges, the mass can be obtained. For a Kevlar tether of $L_0 = 500$ m, the tether has a mass of only 5.2 kg. If the tether's $L_0 = 20$ km, the tether's mass is 208 kg. This is still significantly less that the combined tug-debris mass of 3000 kg and is therefore a reasonable assumption.

Table 4. Material Properties of Tethers Used[8]

Materials	Density [kg/m^3]*	E [GPa]	Max Strength [GPa]	Diameter range [mm]	Area range [m^2]
SPECTRA	970	170	2 - 3	.5 - 3	1.9635e^{-7} - 8e^{-6}
Kevlar	1470	170	2 - 3	.5 - 3	1.9635e^{-7} - 8e^{-6}

Post-Burn Potential Collision Prediction in Deep-Space Scenario

In order to gain a basic understanding of the behavior of the tether system, a deep space (i.e. pure spring-mass dynamics) simulation was run. Insight into the oscillation periods and general

*http://www.matweb.com/index.aspx

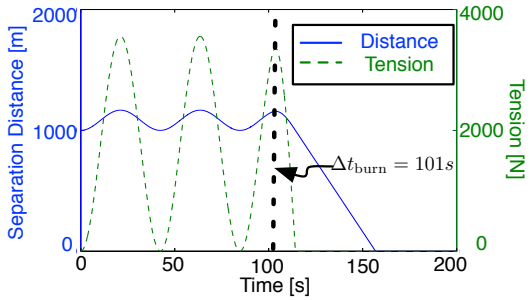

(a) Example motion with E = $3x10^9$ GPa. Collision at 157 s

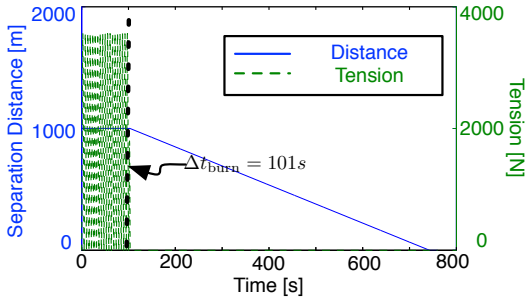

(b) E = $170x10^9$ GPa. Collision at 741 s

Figure 9. Separation distance and tether tension in deep space, $\Delta t_{\text{burn}} = 101$ s, $\Delta v = 120$ m/s. $K_S = 1360$ N/m, T = 5kN

dynamical behavior of the system is obtained through this analysis which is then carried over to the gravity field simulations. In the one-dimensional, deep space analysis, the system behaved much as would be expected from a spring-mass system. During the thrusting period, the two masses separate and often continue expanding for a short time after the burn has stopped. The spring force then pulls the two masses together and without any other forces acting on the system, the masses collide. During constant thrusting collision will not occur. However, the rate it will happen varies depending upon tether length, stiffness, and thrust. All studies run to date show that the collision time is much shorter than the deorbit time. Figures 9 and 10 were obtained using a thrust of 5 kN, the spacecraft values from Table 3, and the tether properties of $E = 170$ GPa, $A = 8e^{-6}$ m^2 with an initial separation distance of $L_0 = 1000$ m between the two masses. Note the cross sectional area was selected because the maximum thrust modeled in this paper is 12 kN and at that force, with a safety factor of 2 and a $\sigma_{\text{max}} = 3$ GPa, an area required is $A = 8e^{-6}$ m^2.

Figure 9 shows two different behaviors, Figure 9(a) with a low Young's Modulus, shows exaggerated motion, and Figure 9(b) to show the actual motion of the tether system. Figure 9(a) demonstrates the periodic motion of both the tether and the tension. When the separation reaches a peak, so does the tension. The velocity at these points are also zero (slope of the separation is zero). Once thrusting stops, remaining tension causes the craft to collapse in on itself. Figure 9(b) behaves similarly however the maximum separation is much smaller, reaching only about 1003 m. The system then begins to collapse upon itself and collision occurs at about 741 seconds. During the thrusting period, it is important to note that the tether tension is always at or above zero. This corresponds

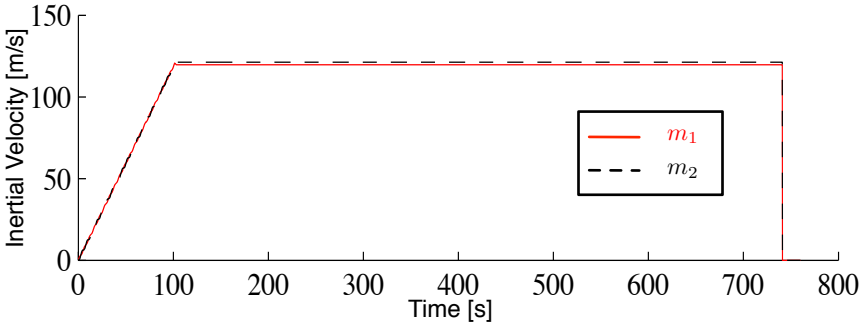

(a) Increase in inertial velocity with tether induced oscillations. $\Delta v = 120$ m/s at 104 s

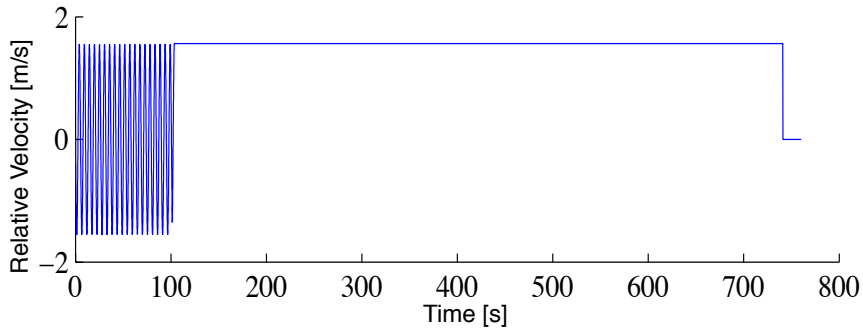

(b) Positive relative velocity means the craft are converging. Equal velocity points at 2.65, 5.3, 7.95, 10.6 ... and 102.3 s.

Figure 10. Velocity of the tether system in deep space showing an eventual collision at 157 s ($K_S = 1360$ N/m). T = 5 kN

to the separation distance always being at, or greater than, L_0. Figure 10 shows the inertial and relative velocity profile of the two masses. The motion of m_1 is almost completely driven by the thrust during the first few seconds before significant tension has built up in the tether. However, due to the high stiffness, m_2 quickly follows m_1 and at approximately 2.65, 5.3, 7.95, and many other points, ending at 102.3 seconds, the two craft are at the same velocity (Figure 10(b)). The 'equal speed points' at 2.65, 7.95... and 104 seconds occur at the same points in time as the maximum separation and tension in Figure 9(a). Because the two craft are no longer expanding, their relative velocity must be zero.

One point of interest is the last 'equal speed point' at about 120 m/s in Figure 10(a). To achieve the desired Δv and the requirement stated above that the masses will not collide, the equal speed point could provide a metric for when to cut the tether. Because the equal speed point occurs at the max separation, the two craft are at relatively large distances from each other. Further, if the tether is cut, the acceleration on both objects will be zero and they will continue at the same relative velocity i.e. zero. This helps to guarantee that collision will not occur. Therefore, the equal speed point would need to be the desired Δv maneuver profile to deorbit both masses. Once this velocity is achieved, the tether could be disconnected and both craft could deorbit safely with minimal risk of collision. It would therefore be of interest to be able to design a maneuver to make the burn time coincide with the desired Δv equal speed point. Starting from Eq. (10), its time derivative can be

taken:

$$\dot{L} = \frac{\frac{T}{m_1}\sin(\sqrt{C}t)}{\sqrt{C}} \tag{12}$$

To find when the relative velocity is zero, $\dot{L} = 0$, the sine expression must be zero. Solving for Δt from Eq. (1) and substituting it into Eq. (12), an expression for the required thrust to make $\dot{L} = 0$ is found. Here n is any integer.

$$T = \frac{\sqrt{C}\Delta v(m_1 + m_2)}{\arcsin 0} = \frac{\sqrt{C}\Delta v(m_1 + m_2)}{n\pi} \tag{13}$$

Using Eq. (13), Figure 11 and Figure 12 were created. Figure 11 uses an n value of 19 while Figure 12 uses an n value of 20. As might be expected, the number of oscillations made during thrusting are directly related to the integer used for n ($20\pi = 10 * 2\pi = 10$ oscillations). Because the system does not start in tension, even n values relate to unstretched tether, equal speed points while odd n values relate to maximum stretch, equal speed points. Thus, Figure 11(a) shows that Δt_{burn} occurs at max tension, and although an equal speed point, a relative velocity is induced by the tether, likely causing the two craft to collide. However, Figure 12(a) shows the Δt_{burn} occurs near zero tension, therefore the relative velocity is near zero and a collision event might only occur after about 2822 seconds. Some slight relative velocity is still present in Figure 12 because the calculated T is for one exact Δt_{burn}. Any numerical errors (integration time step) cause some slight relative velocity. However, it is likely that any relative velocity could be zeroed with control. The major point is: the relative velocity between the two craft can be all but zeroed simply by selection of thrust and/or time of burn, for a given spring-mass system, thus reducing the likelihood of a collision.

Returning to Figure 9(b), the two masses collide after only about 741 seconds, much less than the 45 minutes (2700 seconds) it takes to deorbit. Several sweeps were conducted to determine how tether length could be used to reduce a possible collision event. The times depended upon the thrust, initial separation, 'slack' present in the tether, and the material properties. The more 'slack' in the tether, the longer between a possible collision. However, as will be shown below, 'slack' creates more violent dynamics because the relative velocities between the two craft becomes large. The next section shows that on orbit dynamics significantly increases time for nearest approach, often beyond reentry using separation distances (L_0) of only a few kilometers.

NUMERICAL DEORBIT PERFORMANCE STUDY IN EARTH'S GRAVITY FIELD

With the insight gained from the deep space simulation, the spring-mass system is now placed into a gravity field. In orbit, the tug craft is placed in a trailing, along track position behind the debris. The thrust is directed opposite of the velocity vector. The tether properties used are $E = 170$ GPa, $A = 8e^{-6}$ m^2. Figure 13 shows the separation and altitude profile of both masses. For this simulation the mass properties from Table 3 were used, $T = 5$ kN, $K_S = 68$ N/m, and the required $\Delta v = 120$ m/s. While the initial separation distance is large (20 km), Figure 13 demonstrates the expansion and contraction behavior of the tether system. One very important feature to this system is that it does not collide during the entire 3000 second (50 minute) simulation. In the deep space simulations, it was found that collisions will occur for general thrusts. The orbital motion therefore adds significant acceleration to the system to keep it from colliding, aiding the tether system.

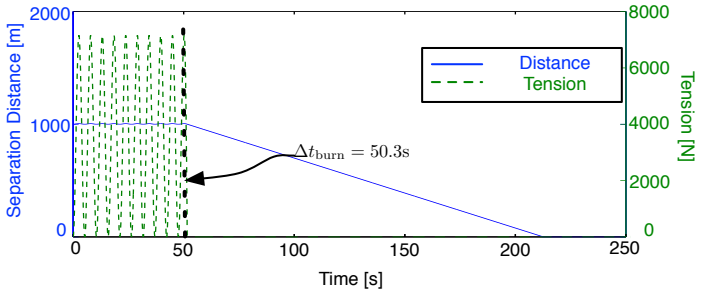

(a) Separation distance and tether tension in deep space. Δt_{burn} = 106s at max tension and separation position.

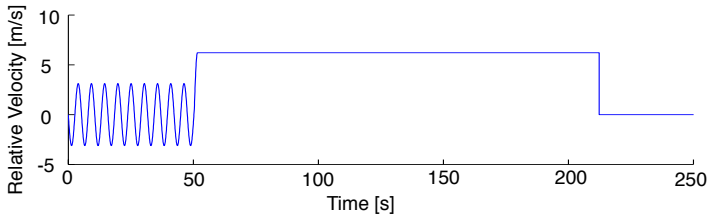

(b) Convergence (positive relative velocity) of craft after Δt_{burn}

Figure 11. Equal speed point and burn time at Δt_{burn} = 50.3 s, with $n\pi = 5\pi$. Collision at 212 s, K_S = 1360 N/m, Δv = 120m/s, T = 10057 N

Utilizing the higher tether material properties from Table 4, and starting at different L_0 values, Figure 14 shows the minimum separation distance achieved for a thrust of $T = 2.5$ kN. No tether slack was present in this simulation. At a separation distance of $L_0 = 500$ m the spring constant is very high, near 2720 N/m, and this helped to create the closest approach between the two craft (a minimum separation of about 118 meters was found, still reasonably large). However, at separation distances larger than 500 m, the craft do avoid collisions, although at $L_0 = 1500$ m, there is another 'close' approach (186 m). This shows that reasonable separation distances may be used for the tether without creating a collision event. The trend of having a large minimum separation was not observed in all simulations run which may point to the fact that the system has varying resonance and other characteristics based upon, L_0, thrust T, K_S, and mass. There may be a significant design space for desirable characteristics with this system.

Figure 15 shows less desirable characteristics at many tether L_0 lengths. Note that the two masses were started at 10 m apart with hundreds or thousands of meters of 'slack' tether between them. A fully expanded tether can slowly build up force as thrust is applied. A slack tether however has a significant impulse as m_1 is traveling at high velocity when the tether has fully unraveled. This produces more violent behavior in the tether dynamics. Figure 15 shows that a slack tether, with the same material properties, thrust and mass as Figure 14 produces six possible collision events compared to Figure 14 zero possible collision events (and only two 'close' passes, more than 100 m in separation).

Figure 16 shows the tension and separation distance behavior on orbit. The tether is in tension only when the separation distance is greater than the initial L_0 value and again, the peaks in tension occur at the maximum separation distances, just like in the deep space simulation. The thrust adds

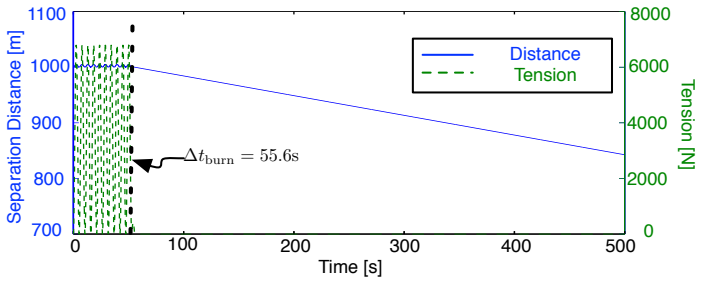

(a) Separation distance and tether tension in deep space. Δt_{burn} = 127s at zero tension and a separation of L_0.

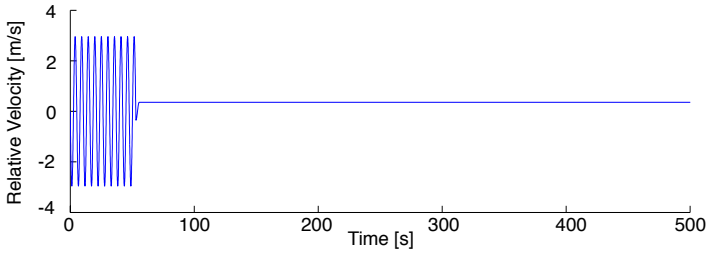

(b) Near zero relative velocity of craft after Δt_{burn}

Figure 12. Equal speed point and burn time at Δt_{burn} = 55.6 s, with $n\pi = 20\pi$. Collision at 2822 s, K_S = 1360 N/m, Δv = 120m/s, T = 9554 N

tension to the tether, which then acts like a spring and pulls the two craft back together. Once the thrust stops, the differential gravity experienced by the satellites at different altitudes (Figure 13) puts the tether back in tension. Thus the system can oscillate both before and after thrusting occurs, unlike the deep space simulations.

Similarly to the deep space simulation, Eq. (13) is used to find the ideal thrust that provides nearly zero relative velocity between the two craft. Using the same material properties and L_0 as Figure 16 and $n = 30$ from Eq. (13), Figure 17 is obtained. Interestingly, the relative separation distance does not remain as constant after thrusting, at the initial $L_0 = 1500$ m, as expected. However, the gross separation throughout the orbit is reduced as shown in Figure 18(b). Comparing the motion of the $T = 2.5$ kN to the thrust of $T = 5201$ N that produces the reduced relative velocity over two orbits, the differences can be seen. Figure 18(a) shows that the $T = 2.5$ kN will cause lower separation distances to occur compared to the desirably throttled motion in Figure 18(b) which never passes below 200 m in separation distance. At the first periapses, around 3000 seconds, both thrust profiles produce local minimum separation distances due to the higher speeds and orbital dynamics 'compressing' the formation. However, after this point reasonably large separation distances are maintained in Figure 18(b), even at the next periapses passage at around 8000 seconds. Conversely, several lower separation distances occur in Figure 18(a). Further, the time of one of the closest approaches for Figure 18(b) is at periapses, or where the two craft are expected to burn up.

Increasing the minimum separation distance is another way to avoid collisions with this system. However the minimum separation distance is dependent upon the thrust (T), the material properties (E, A), the masses, the initial separation distance, and the nominal tether length (L_0). Sweeping

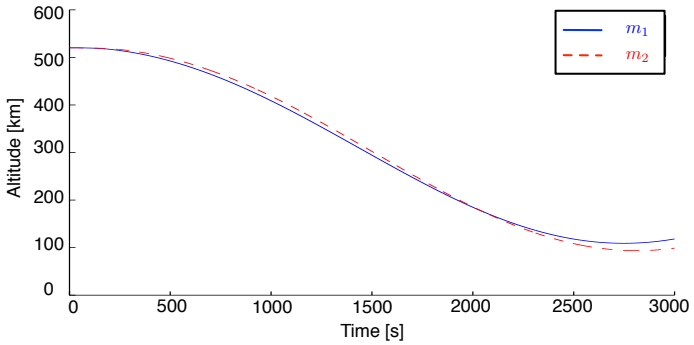

Figure 13. De-orbit altitude profile for $L_0 = 20$ km ($K_S = 68$ N/m) and $T = 2.5$ kN

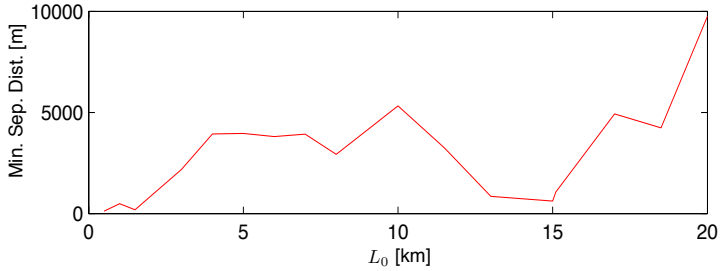

Figure 14. Initial tether length's (L_0) affect on minimum separation distance between each body ($T = 2.5$ kN) in orbit

over thrust and initial separation distances set to L_0, Figure 19 was obtained for the mass properties given in Table 3. Figure 19 is an expanded plot of Figure 14 across multiple thrusts. Figure 19(a) and Figure 19(b) display the same data. Figure 19 shows that the general trend between the two craft is that low thrusts and large L_0 values increase the minimum separation. This intuitively makes sense because lower thrusts put less energy into the tether and therefore there is less spring force and potential to pull the two craft near each other. Still, Figure 19 is not a simple surface and there appear to be many local peaks. These peaks may correspond to resonances between the tether system and the orbital motion. The peaks may also be locations where the thrust is throttled to produce nearly zero relative velocity between the craft, like in Figure 17. Also interestingly, it seems that as initial separation distance (L_0) increases minimum separation distance increases, almost independent of thrust. The cause of peaks is a topic for future work.

The thrust possibly provided by the Soyuz of about 2 kN is shown by the dotted line on Figure 19(b). This thrust magnitude crosses several peaks and generally maintains reasonable separation distances, making this a good thrust to use. Tether lengths of $L_0 = 500$ and $L_0 = 1000$ m should be avoided because they often produce the smallest separation distances. It should be noted that generally, minimum separation distances are in the hundreds to thousands of meters and therefore the likelihood of collision is small. Figure 19 shows that the tether debris removal system is usable for most thrust - L_0 regimes and therefore this system appears feasible.

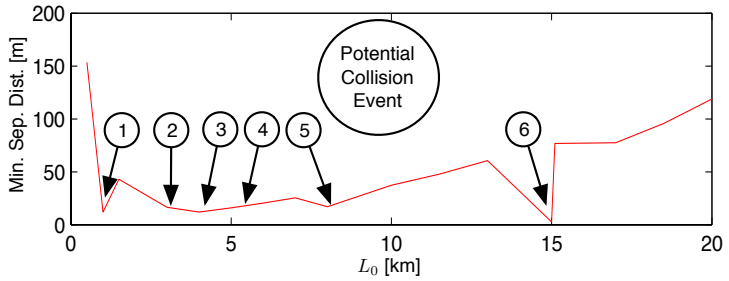

Figure 15. Minimum separation distance achieved given an initial separation of 10 m, with a specified L_0 and $(L_0 - 10)$ m of slack, in orbit. 'Collision' at any point less than 20 m separation.

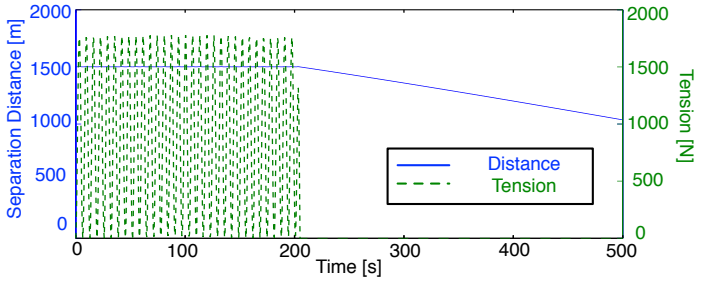

Figure 16. Separation distance and tether tension in orbit for the first 500 seconds ($K_S = 906.7$ N/m), $T = 2.5$ kN, and $\Delta t_{\text{burn}} = 202$ s

CONCLUSION

A tethered rocket-debris system is a conceptually viable debris removal system for low Earth Orbits. The residual fuel reserves of a launch vehicle upper stage is used to rendervouz with the larger rocket debris, and deorbit both objects at once. The new launch system serves a dual purpose of delivering a payload to space, and then deorbiting a large debris object with similar orbit parameters. Using only approximately $\Delta v = 100$ m/s moves a Cosmos-3M from an 800 km orbit into one that will decay within 25 years. At lower altitudes or with more fuel the tethered debris removal system could completely deorbit within a very short time frame. This indicates that rocket stages with excess fuel can be made into debris deorbiters. The tethered debris system has a significant design space where collisions between the rocket and debris can be avoided while significant Δv can be added to the system to deorbit both objects effectively. Choosing an appropriate thrust value can ensure thrust termination at a local relative speed and tether tension minimum. This reduces the possibility of collision. Future studies of this system will consider enhanced tether models (tether with mass), the attitude of the tug and debris objects, and further explore the T - L_0 trade space. The system can also be throttled to achieve zero relative velocity and tether tension to reduce collisions between both craft. Using present day tether materials and rocket technologies it is very feasible to use this system as an active debris removal system.

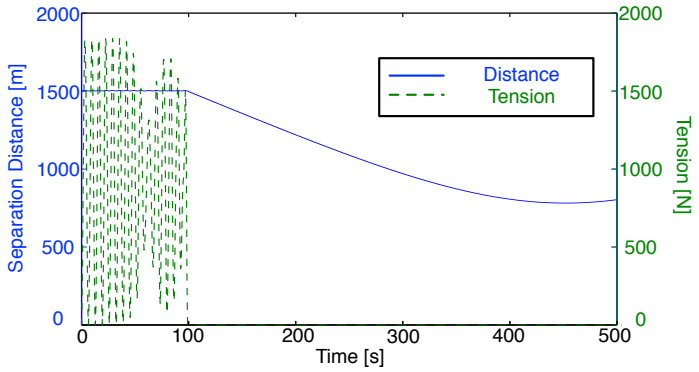

Figure 17. Separation distance and tether tension in orbit for the first 500 seconds to reduce relative velocity ($K_S = 906.7$ N/m), $T = 5201$ kN, and $\Delta t_{\text{burn}} = 97.3$ s

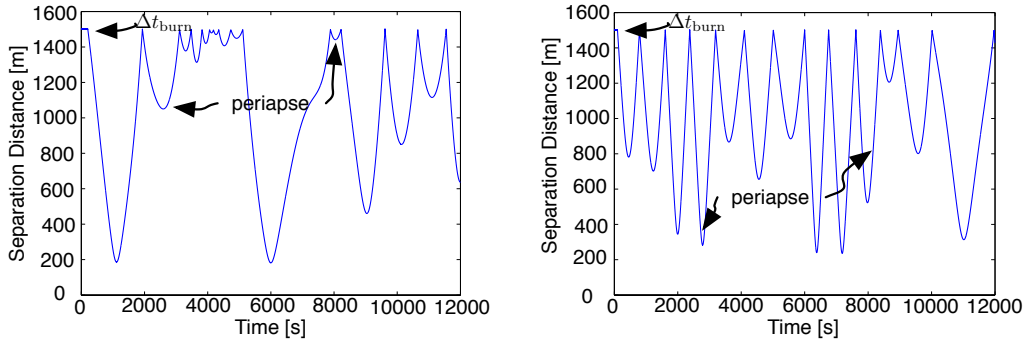

(a) Generic $T = 2.5$ kN, $\Delta t_{\text{burn}} = 202$ s.

(b) Thrusting to reduce relative velocity. $n = 30$, $T = 5201$ kN, $\Delta t_{\text{burn}} = 97.3$ s.

Figure 18. Separation distance over two orbits for a generic thrust value and a thrust designed to reduce relative velocity. The desired $\Delta v = 120$ m/s

REFERENCES

[1] T. Kelso, "Analysis of the 2007 Chinese ASAT Test and the Impact of its Debris on the Space Environment," *Center for Space Standards & Innovation*, Maui, Hawaii, 2007, pp. 321–330.

[2] D. J. Kessler and B. G. Cour-Palais, "Collision Frequency of Artificial Satellites: The Creation of a Debris Belt," *Geophysical Research*, Vol. 83, No. A6, 1978, pp. 2637–2646.

[3] N. L. Johnson, "Orbital Debris: The Growing Threat to Space Operations," *33rd Annual AAS Guidance and Control Conference*, Breckenridge, CO, Feb. 6–10 2010.

[4] J.-C. Liou, N. Johnson, and N. Hill, "Controlling the growth of future LEO debris populations with active debris removal," *Acta Astronautica*, Vol. 66, No. 5-6, 2010, pp. 648 – 653.

[5] J. A. Carroll, "Tether Applications in Space Transportation," *Acta Astronautica*, Vol. 13, No. 4, 1986, pp. 165–174.

[6] M. P. Cartmell and D. J. McKenzie, "A Review of Space Tether Research," *Elsevier Progress in Aerospace Sciences*, Vol. 44, 2008, pp. 1–21.

[7] R. D. E. L. Johnson, B. Gilchrist and E. Lorenzini, "Overview of Future NASA Tether Applications," *COSPAR Advanced Space Research*, Vol. 24, No. 4, 1985, pp. 1055–1063.

[8] J. A. Carroll and J. C. Oldson, "Tethers for Small Satellite Applications," *AIAA/USU Small Satellite Conference*, Logan, Utah, 1995.

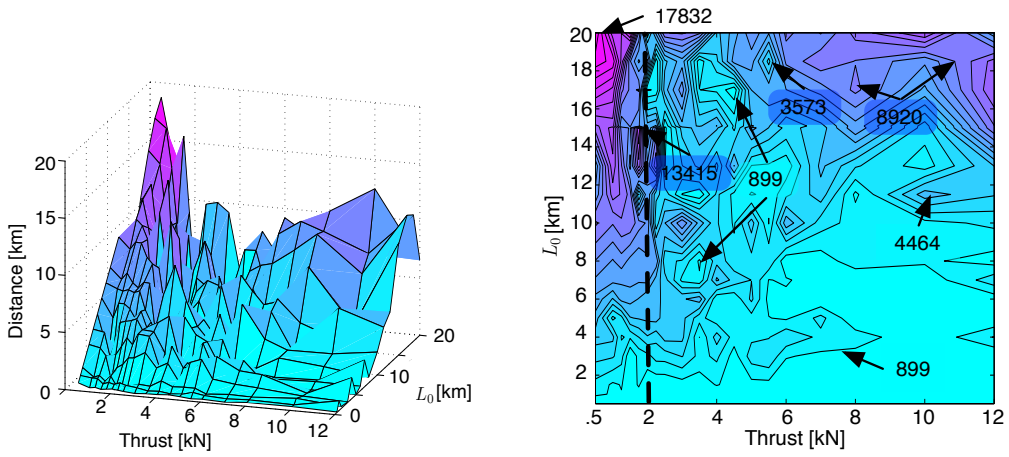

(a) Minimum Separation Distance

(b) $T = .5 - 7$ kN. All contours in meters. Dotted line is approximate thrust of Soyuz.

Figure 19. Surface and Contour plots for minimum craft separation distance using a range of L_0 (K_S) and thrust. E = 170 GPa and A = 8x10^{-6} m^2

[9] K. Heiner, *Space Debris: Models and Risk Analysis*. Chichester, UK: Springer-Praxis, 1st ed., 2006.

[10] J.-C. Liou, "An active debris removal parametric study for LEO environment remediation," *Advances in Space Research*, Vol. 47, No. 11, 2011, pp. 1865 – 1876.

[11] J.-C. Liou, "Active Debris Removal – A Grand Engineering Challenge for the Twenty-First Century," *AAS Spaceflight Mechanics Meeting*, New Orleans, LA, Feb. 13–17 2011.

[12] N. M. Ivanov and L. N. Lisenko, "Ballistic and Navigation of Space Vehicles," *Drofa*, Moscow, Russia, 2004.

[13] V. Serduk, *Designing of Space Launch Vehicles*. Moscow, Russia: Mashinostroenie, 2009.

[14] W. J. Larson and J. R. Wertz, *Space mission: Analysis and Design*. Microcosm Inc., 3rd ed., 1999.

[15] V. S. Syromyatnikov, *Docking Devices of Spacecraft*. Moscow, Russia: Mashinostroenie, 1984.

[16] M. H. Kaplan, "Space debris realities and removal," *SOSTC Improving Space Operations Workshop*, Goddard Space Flight Center, Greenbelt, Maryland, May 25 2010.

[17] E. Perez, *SOYUZ from the Guiana Space Centre User's Manual*. Arianespace, Evry-Courcouronnes Cedex, France, 1 ed., June 2006.